OPTICAL BISTABILITY IN A DEGENERATE TWO-LEVEL EIT MEDIUM UNDER THE INFLUENCE OF AN EXTERNAL MAGNETIC FIELD: AN ANALYTICAL APPROACH

Le Thi Minh Phuong[a], Dinh Xuan Khoa[b], Nguyen Huy Bang[b], Thai Doan Thanh[c], Nguyen Tuan Anh[c], Nguyen Thi Thu Hien[c], Hoang Minh Dong[c*]

[a]The Faculty of Natural Sciences Pedagogy, Saigon University, Ho Chi Minh City, Vietnam
[b]The Department of Physics and Techonology, Vinh University, Nghe An, Vietnam
[c]The Faculty of Applied Sciences, Ho Chi Minh City University of Food Industry, Ho Chi Minh City, Vietnam
[*]Corresponding author: Email: dong.gtvtmt@gmail.com

Article history
Received: March 15th, 2021
Received in revised form (1st): May 19th, 2021 | Received in revised form (2nd): May 27th, 2021
Accepted: May 29th, 2021
Available online: July 22nd, 2021

Abstract

We investigate the behavior of optical bistability in a degenerate two-level atomic medium using an external magnetic field to separate the lower level into two distinct levels that both connect to an upper level by the probe and coupling laser fields. Based on analytical solutions, the absorption spectrum and behavior of optical bistability in an electromagnetically induced transparency regime under an external magnetic field are investigated. By controlling the external magnetic field, we find that the appearance and disappearance of the optical bistability can be easily controlled according to the strength of the magnetic field in the transparent window domain. Furthermore, the effects of the intensity of the coupling laser field and the parameters of the system on the behavior of optical bistability are also considered. The proposed model is useful for applications in all-optical switches and magneto-optic storage devices.

Keywords: Analytical solution; Electromagnetically induced transparency; External magnetic field; Optical bistability.

DOI: http://dx.doi.org/10.37569/DalatUniversity.11.4.872(2021)

Article type: (peer-reviewed) Full-length research article

1. INTRODUCTION

In recent decades, quantum coherence and interference in atomic systems have played a major role in transforming the optical properties of media because of their potential applications in nonlinear optics. Recently, the discovery of the electromagnetically induced transparency (EIT) effect (Boller et al., 1991) has led to investigations into many amazing phenomena, such as lasing without population inversion (Zibrov et al., 1995), ultra-slow light propagation (Hoang et al., 2020; Hau et al., 1999), optical bistability, and all-optical switching (Joshi & Xiao, 2012).

Optical bistability (OB) has been greatly developed because of potential applications in all-optical switching and optical transistors, which are essential elements in quantum computers and quantum information. Optical bistability has been widely studied both theoretically and experimentally in different atomic media (Gibbs et al., 1976; Joshi & Xiao, 2012; Rosenberger et al., 1983). Most of the OB studies have examined systems of two-level atoms in an optical resonance cavity (Gibbs et al., 1976; Rosenberger et al., 1983). However, due to the passive nature of two-level atomic models, OB can only be controlled by varying the intensity of the input signal beam, which is also the signal received at the output. Consequently, multilevel atomic systems have also been proposed to investigate the behavior of optical bistability and optical multibistability in atomic systems (Brown et al., 2003; Haifeng, 2019; Jafarzadeh et al., 2014). The remarkable advantage of the multilevel system compared to the two-level system is the creation of a nonlinear medium inside an optical cavity capable of inducing atomic coherence, which can significantly change the absorptivity, dispersion, and nonlinearity of the medium (Brown et al., 2003). Furthermore, it has been shown in some studies that the optical properties of multilevel atomic systems can be controlled by coherent control fields. In this case, quantum coherence and quantum interference are the fundamental mechanisms for altering the optical responses of the medium. On the basis of these studies, Harshawadhan and Agarwal (1996) demonstrated that quantum coherence and interference can significantly reduce the threshold intensity of the OB. Gong et al. (1997) showed that large OB widths could be achieved if the initial coherence of a three-level atomic system was enhanced. Moreover, there are several methods for the generation of all-optical switching based on multiple cascaded resonators with reduced switching intensity-response time products (Ngo, Kim et al., 2012) and optical bistability based on guided-mode resonances (Ngo, Le et al., 2012) in photonic crystal slabs. These studies have shown that the performance of optically bistable devices can be evaluated through a switching intensity-response time product. And nonlinear characteristics, such as switching intensity and switching time, are suggested as performance metrics for all-optical switches. Joshi, Brown et al. (2003) have experimentally studied OB behavior in a three-level Rb atomic system connected by a strong coherent field and a linearly polarized weak-beam. Their work has shown that OB can be easily controlled by the strength of the control field and frequency detuning. In addition, the effects of quantum interference and the relative phase of the applied fields (Gong et al., 1996; Joshi, Yang et al., 2003) and spontaneously generated emission (Cheng et al., 2004) on OB have also been studied. More recently, the behavior of OB and multistability under the influence of an external magnetic field and the polarization of the coupling laser fields has been also

investigated (Asadpour & Soleimani, 2014; Hoang et al., 2019; Zhang et al., 2013). In this direction, most research projects use numerical methods, and there is a lack of research on analytical solutions for OB. The analytical approach makes it easy to examine quantitative parameters of the laser system and is advantageous in comparison with experimental parameters.

In this paper, we use an analytical approach to study OB in a degenerate two-level atomic system under the EIT effect of an external magnetic field. It is shown that the bistable behavior can be controlled by adjusting the external magnetic field, the intensity of the coupling field, and parameters of the system. The paper focuses on controlling intensity switching based on steady-state medium responses. Therefore, within the scope of our research, the switching time and the performance of switching types are not considered; these can be found in more extensive studies, such as Anh et al. (2021), Hoang & Nguyen (2019), and Ngo, Kim et al. (2012). The proposed model can be useful in all-optical switching, logic gates, and optical-magnetic memory applications. Furthermore, the model is easy to realize in an experiment because the system can be performed in different frequency regimes using only a single laser for both coupling and probe fields.

2. MODEL AND BASIC EQUATIONS

Consider a degenerate two-level atomic system under the influence of an external magnetic field, as shown in Figure 1a. A right circularly polarized σ^+ control laser field with Rabi frequency $\Omega_c = \mu_{23}E_c / 2\hbar$ couples levels $|3\rangle \leftrightarrow |2\rangle$ while a left circularly polarized σ^- weak probe laser field with Rabi frequency $\Omega_p = \mu_{21}E_p / 2\hbar$ couples levels $|1\rangle \leftrightarrow |2\rangle$. Under the influence of the external magnetic field the $|1\rangle$ and $|3\rangle$ levels undergo a Zeeman shift by a distance $\Delta_B = \mu_B m_F g_F B / \hbar$, where μ_B is the Bohr magneton coefficient, g_F is the Landé factor, and $m_F = \pm 1$ is the magnetic quantum number of the corresponding state. The decay rates from states $|2\rangle$ to $|1\rangle$ and $|2\rangle$ to $|3\rangle$ are given by γ_{21} and γ_{23}, respectively. The relaxation rate of coherence between ground states $|1\rangle$ and $|3\rangle$ by collisions is negligible.

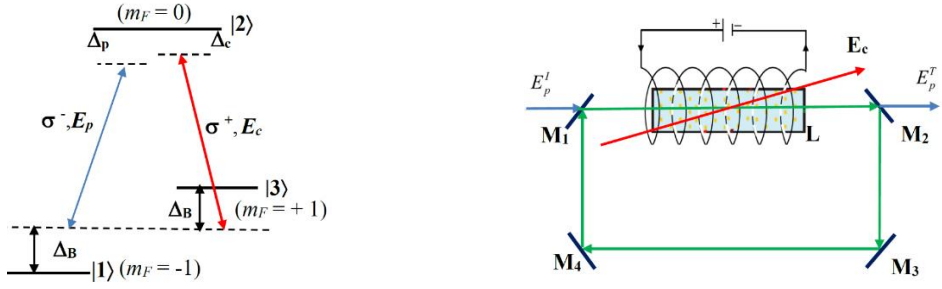

(a) (b)

Figure 1. (a) The degenerate two-level atomic model under the influence of control, probe, and external magnetic fields; (b) Unidirectional ring cavity containing an atomic sample of length *L*

Note: E_p^I and E_p^T are the incident and transmission fields, respectively.

In the rotating-wave and electric dipole approximations, the total Hamiltonian describing the atom-field interaction of the system can be written (assuming $\hbar = 1$):

$$H_{\text{int}} = \left(\Delta_p + \Delta_B\right)\left|2\right\rangle\left\langle 2\right| + \left(\Delta_p - \Delta_c + 2\Delta_B\right)\left|3\right\rangle\left\langle 3\right| - \left(\Omega_p\left|2\right\rangle\left\langle 1\right| + \Omega_c\left|3\right\rangle\left\langle 2\right| + H.c\right), \quad (1)$$

where $\Delta_p = \omega_{21} - \omega_p$ and $\Delta_c = \omega_{23} - \omega_c$ are detunings of the probe field and coupling field from the atomic transition frequencies, respectively.

The dynamic evolution of the system is described by the Liouville equation:

$$\frac{\partial \rho}{\partial t} = -i\left[H_{\text{int}}, \rho\right] + \Lambda\rho \ , \quad (2)$$

The density matrix equations for this system can be written as:

$$\dot{\rho}_{11} = \gamma_{31}\left(\rho_{33} - \rho_{11}\right) + \gamma_{21}\rho_{22} + i\Omega_p\rho_{21} - i\Omega_p\rho_{12} \ , \quad (3a)$$

$$\dot{\rho}_{22} = -\left(\gamma_{21} + \gamma_{23}\right)\rho_{22} + i\Omega_p\rho_{12} - i\Omega_p\rho_{21} + i\Omega_c\rho_{32} - i\Omega_c\rho_{23} \ , \quad (3b)$$

$$\dot{\rho}_{33} = -\gamma_{31}\left(\rho_{33} - \rho_{11}\right)\gamma_{23}\rho_{22} + i\Omega_c^*\rho_{23} - i\Omega_c\rho_{32} \ , \quad (3c)$$

$$\dot{\rho}_{21} = -(i\left(\Delta_p + \Delta_B\right) + \gamma)\rho_{21} - i\Omega_p(\rho_{22} - \rho_{11}) + i\Omega_c\rho_{31} \ , \quad (3d)$$

$$\dot{\rho}_{31} = -\left(\gamma_{31} + i\left(\Delta_p - \Delta_c + 2\Delta_B\right)\right)\rho_{31} - i\Omega_p\rho_{32} + i\Omega_c^*\rho_{21} \ , \quad (3e)$$

$$\dot{\rho}_{23} = -\left(i\left(\Delta_c - \Delta_B\right) + \gamma\right)\rho_{23} - i\Omega_c\left(\rho_{22} - \rho_{33}\right) + i\Omega_p\rho_{13}, \quad (3f)$$

where, $\rho_{ij} = \rho_{ji}^*$ (i, j = 1, 2, 3; $i \neq j$), $\rho_{11} + \rho_{22} + \rho_{33} = 1$, $\gamma = \left(\gamma_{21} + \gamma_{23} + \gamma_{31}\right)/2$, and γ_{ij} is the decay rate between levels $|i\rangle$ and $|j\rangle$, respectively.

Now, we put the ensemble of *N* degenerate two-level atoms into a unidirectional ring cavity, as shown in Figure 1b. For simplicity, we assume that mirrors 3 and 4 have 100% reflectivity; the reflection and transmission coefficient of mirrors 1 and 2 are *R* and T (with *R* + *T* = 1), respectively. The total electromagnetic field has the form: $E = E_p e^{-i\omega_p t} + E_c e^{-i\omega_c t} + c.c.$, where only the probe field E_P is circulating in the ring cavity. In the slowly varying envelope approximation, the dynamic response of the probe field is governed by Maxwell's equations:

$$\frac{\partial E_p}{\partial t} + c\frac{\partial E_p}{\partial z} = i\frac{\omega_p}{2\varepsilon_0}P\left(\omega_p\right), \quad (4)$$

where c and ε_0 are the light speed and permittivity in free space, respectively. $P\left(\omega_p\right)$ is the induced polarization in transition $|1\rangle \leftrightarrow |2\rangle$:

$$P\left(\omega_p\right) = N\mu_{21}\rho_{21}, \tag{5}$$

where μ_{21} is the electric dipole moment, and ρ_{21} is the density matrix element. Substituting Equation (5) into Equation (4), we have the relationship between the light field amplitude and density matrix element:

$$\frac{\partial E_p}{\partial z} = i\frac{N\mu_{21}\omega_p}{2c\varepsilon_0}\rho_{21}. \tag{6}$$

For a perfectly tuned ring cavity, the boundary conditions in the steady-state limit between the incident field E_p^I and the transmitted field E_p^T are:

$$E_p\left(L\right) = E_p^T/\sqrt{T}, \tag{7a}$$

$$E_p\left(0\right) = \sqrt{T}E_p^I + RE_p\left(L\right), \tag{7b}$$

where L is the atomic sample length, and R is the feedback mechanism due to the reflection from mirror M_2 responsible for the bistability behavior, i.e., no bistability can occur if $R = 0$. In the mean-field limit, using the boundary conditions and Equation (4), and normalizing the fields by letting $y = \mu_{21}E_p^I/\hbar\sqrt{T}$ and $x = \mu_{21}E_p^T/\hbar\sqrt{T}$, we can obtain the input-output relationship

$$y = x - iC\rho_{21}, \tag{8}$$

where $C = \omega_p L\left|\mu_{21}\right|^2 N/2\hbar\varepsilon_0 cT$ is the usual cooperation parameter for atoms in a ring cavity. The analytical solution for the density matrix element ρ_{21} is obtained by solving the system of Equations (3) in the steady state. Details are given in the appendix. From Equation (8), we study the input-output behavior of the bistability, which will be presented in the following section.

3. RESULTS AND DISCUSSION

We apply the model for the cold atomic medium ^{87}Rb using the 5S-5P transitions as a realistic candidate. The states $|1\rangle$, $|2\rangle$, and $|3\rangle$ can be selected as follows: $5S_{1/2}$ ($F = 1$, $m_F = 1$), $5P_{1/2}$ ($F = 1$, $m_F = 0$), and $5S_{1/2}$ ($F = 1$, $m_F = -1$), respectively. All atoms are assumed to be optically pumped to the states $|1\rangle$ and $|3\rangle$, which therefore have the same incoherent populations equal to 1/2, i.e., $\rho_{11} = \rho_{33} = 1/2$ (Hoang et al., 2019). The decay rate $\gamma_{21} = \gamma_{23} = 2\pi$ x 5.3 MHz, and the wavelength of the probe and control lasers is $\lambda_p = \lambda_c = 795$ nm. The Landé coefficient is $g_F = -1/2$ and the Bohr magneton is $\mu_B = 9.27401 \times 10^{-24}$ JT^{-1} (Steck, 2019). Here, the Zeeman shift Δ_B is taken in units of the decay rate γ_{21}, so the strength of the magnetic field B is calculated in terms of the unit of the combined constant $\gamma_c = \hbar\mu_B^{-1}g_F^{-1}\gamma_{21}$.

First, we analyzed the influence of the magnetic field B on the threshold and width of the OB. Figure 2a shows that the threshold of optical bistability first increased significantly, and the threshold width became wider as the intensity of the external magnetic increased but then decreased gradually although the intensity of the external

magnetic field continued to increase. To clarify this phenomenon, we plotted the probe absorption coefficients Im (ρ_{21}) according to the strength of the magnetic field B, as shown in Figure 2b. When the magnetic field B is absent (i.e., $B = 0$), levels $|1\rangle$ and $|3\rangle$ are identical, the absorption of the medium is maximumly degrading under the EIT condition, and there is no OB. However, when the magnetic field is turned on (i.e., $B \neq 0$), the Zeeman level splitting between levels $|1\rangle$ and $|3\rangle$ is enhanced with the increase in strength of the magnetic field. Hence, the quantum interference between the two transition channels $|1\rangle \leftrightarrow |2\rangle$ and $|3\rangle \leftrightarrow |2\rangle$ is attenuated, which increases the absorption of the probe laser beam. When the external magnetic field B increases to the value $B = 3.5\gamma_c$, the probe absorption reaches a maximum value (shown as the red star in Figure 2b), and the bistable threshold reaches the maximum. If B continues to increase, the amplitude of the probe absorption spectrum is decreased sharply and eventually reaches a small stable value close to zero, leading the bistable threshold to decrease slowly. Thus, by choosing the proper strength of the magnetic field, we can switch the medium from light-absorbing to completely transparent and vice versa. Therefore, the threshold value and the width of the OB can be controlled by adjusting the magnetic field to the appropriate value.

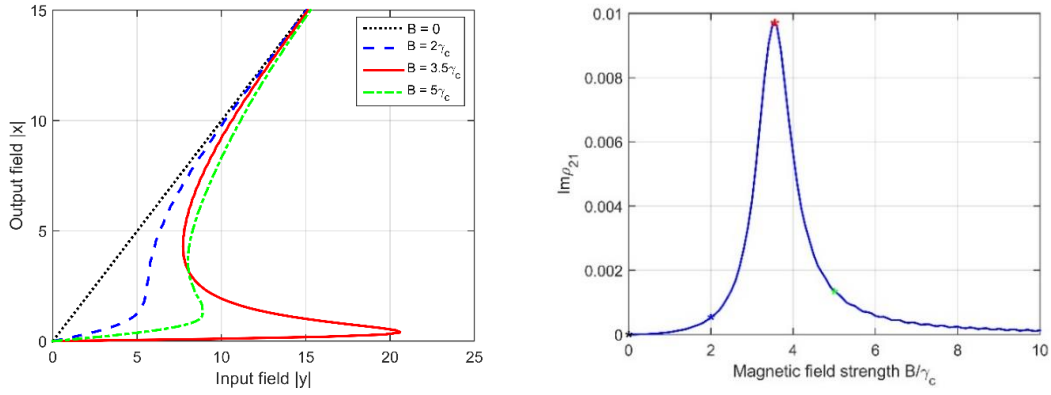

(a) (b)

Figure 2. (a) Plots of the input-output field curves for different values of the magnetic field B; (b) the variation of the probe absorption spectrum versus magnetic field strength

Note: Other parameters are selected as: $\Omega_p = 0.01\gamma_{21}$, $\Omega_c = 5\gamma_{21}$, $\Delta_c = \Delta_p = 0$ and $\gamma_{23} = \gamma_{21}$, respectively.

In Figure 3 we show the dependence of the OB characteristics on the intensity of the controlling laser field Ω_c. From Figure 3a we see that the bistable threshold increases as the intensity of the control laser field increases and then decreases significantly. Indeed, when the control laser field Ω_c increases from $1\gamma_{21}$ to a value in the neighborhood of $\Omega_c = 5\gamma_{21}$, the probe absorption reaches the saturation value, and the OB threshold can reach the maximum value (the solid red line in Figure 3a). However, as Ω_c continues to increase, the bistable threshold decreases rapidly. It can be easily explained that an increased control field strength will dramatically reduce the absorption for the probe field in the transition from $|2\rangle$ to $|1\rangle$ and enhance nonlinearity of the medium, which leads to the change of the OB behavior that is also evident in Figure 3b. Thus, we can control the threshold intensity of the OB by adjusting the strength of the control field Ω_c.

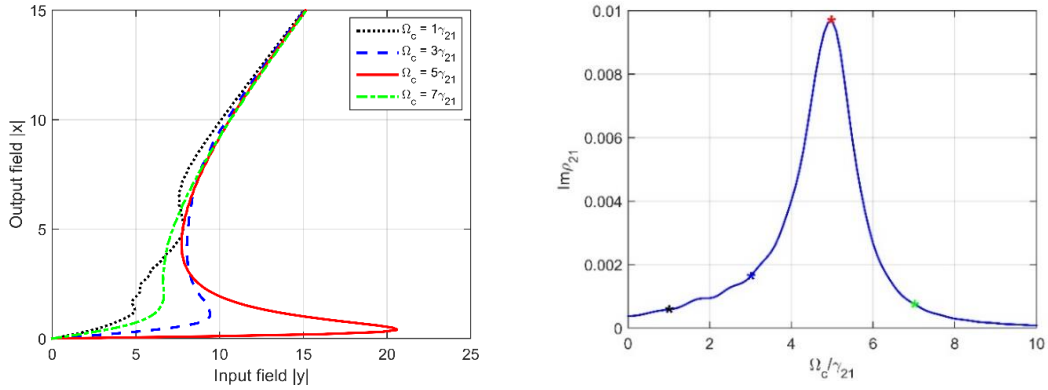

(a) (b)

Figure 3. (a) Plots of the input-output field curves for different values of the coupling field Ω_c; (b) the variation of the probe absorption spectrum versus coupling field intensity Ω_c

Note: Other parameters are selected as: $\Omega_p = 0.01\gamma_{21}$, $\Delta_c = \Delta_p = 0$, $C = 200$, $B = 3.5\gamma_c$ and $\gamma_{23} = \gamma_{21}$, respectively.

Up to now, we have proved the presence of OB in the present atomic system. However, one of the most important system parameters, the detuning of the probe field Δ_p, can also be used to control the position of the EIT window. In Figure 4, we present the behavior of OB via the detuning adjustment of the probe field Δ_p at different values of the magnetic field B. Figure 4a clearly shows that as the frequency detuning Δ_p increases from 0 to $5\gamma_{21}$, the bistability threshold gradually decreases. This can be explained based on the results shown in Figure 4b. With $\Delta_p = 0$ (corresponding to $B = 2$), the probe absorption is the largest, and when shifting to the left on the frequency axis, the probe absorption is decreased due to moving closer to the center of the EIT window. At $\Delta_p = 5\gamma_{21}$ the absorption of the probe field is minimal, and we barely obtain OB.

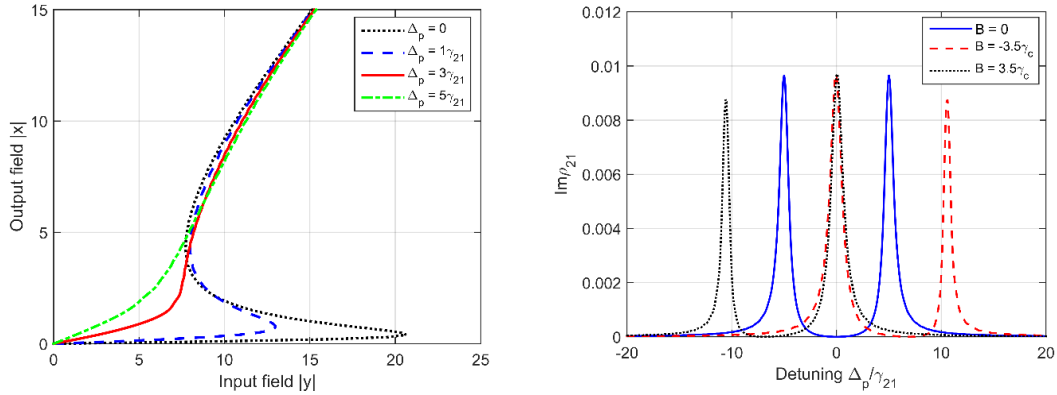

(a) (b)

Figure 4. (a) Plots of the input-output field curves for different values of probe detuning Δ_p; (b) the variation of the probe absorption spectrum versus probe detuning of the magnetic field B

Note: Other parameters are selected as: $\Omega_p = 0.01\gamma_{21}$, $\Omega_c = 5\gamma_{21}$, $\Delta_c = 0$, $B = 3.5\gamma_c$ and $\gamma_{23} = \gamma_{21}$, respectively.

Finally, we display the dependence of the OB curves on the atomic cooperation parameter *C*. Figure 5 shows that the OB threshold increases with the increase of the atomic cooperation parameter *C*. Physically, an increase of the OB threshold versus parameter C is shown clearly through $C = \omega_p L|\mu_{21}|^2 N / 2\hbar\varepsilon_0 cT$. Here we can see that the cooperation parameter *C* is proportional to the atomic number density *N*. Thus, as the atomic number density increases, the sample absorption to the probe field is increased due to the OB threshold increase when the atomic cooperation parameter *C* is increasing.

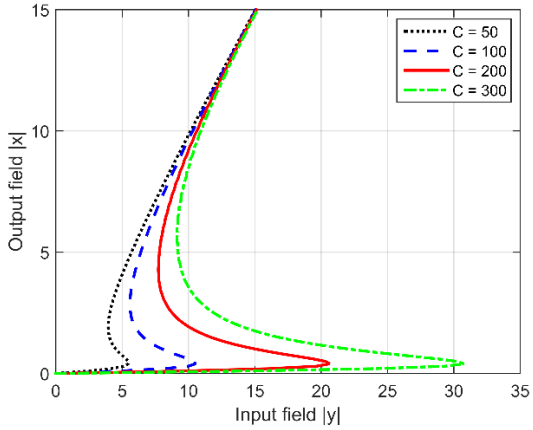

Figure 5. Plots of the input-output field curves for different values of the cooperation parameter *C*

Note: Other parameters are selected as: $\Omega_c = 5\gamma_{21}$, $\Delta_c = \Delta_p = 0$, $B = 3.5\gamma_c$, and $\gamma_{23} = \gamma_{21}$, respectively.

Before ending this paper, we discuss a possible experimental realization for the case of ^{87}Rb atoms on $5S_{1/2} \leftrightarrow 5P_{1/2}$ transitions (Yan et al., 2001). The excitation scheme and experiment can be arranged as in Figure 1. Here, the states $|1\rangle$, $|2\rangle$, and $|3\rangle$ are given as $5S_{1/2}$ ($F = 1$, $m_F = -1$), $5S_{1/2}$ ($F = 1$, $m_F = 1$), and $5P_{1/2}$ ($F = 1$, $m_F = 0$), respectively. When taking the Zeeman shift $\Delta_B = 2\gamma_{21} = 2\times 2\pi \times 5.3$MHz for $5S_{1/2}$ in our calculations, according to the relationship $\Delta_B = \mu_B m_F g_F B/\hbar$, with the magnetic quantum number m = -1, the Landé coefficient g_F = -1/2, and Bohr magneton μ_B = 9.27401 x 10^{-24} JT^{-1}, the magnetic field strength $B = 2\gamma_c \simeq 1.5\times 10^{-3}$T = 15 G is needed and can be easily fulfilled in the experiment. Before interacting with atoms, both the weak probe and control laser fields can be used in combination with a single-mode external cavity diode laser (795 nm) with a beam diameter ≈ 0.8 mm and output power ≈ 1 mW. Due to the Zeeman splitting in opposite directions for the levels $5S_{1/2}$ ($F = 1$, $m_F = -1$) and $5S_{1/2}$ ($F = 1$, $m_F = +1$), and to ensure selection rules for the excitation configuration, the coupling and probe beams are directed to quarter-wave plates to produce σ^- (probe beam) and σ^+ (coupling) polarized beams.

4. CONCLUSIONS

In this paper, we have studied the behavior of optical bistability in a degenerate two-level atomic medium under the influence of an external magnetic field and the EIT effect. The results show that the threshold and width of the OB are easily controlled by

modulating the strength of the magnetic field in different spectral regions of the probe field. Turning a magnetic field on or off can lead to the appearance or disappearance of the OB. In addition, the characteristics of the OB are also controlled by the coupling laser field intensity, frequency probe detuning, and the atomic cooperation parameters of the system. The proposed model is useful for creating all-optical and optical-magnetic switches for applications in optical communications.

ACKNOWLEDGMENT

This work was sponsored and funded by Ho Chi Minh City University of Food Industry under Contract Nos. 148/HD-DCT and 62/HD-DCT and Saigon University under Contract No. 941/HĐ-ĐHSG.

REFERENCES

Anh, N. T., Thanh, T. D., Bang, N. H., & Dong, H. M. (2021). Microwave-assisted all-optical switching in a four-level atomic system. *Pramana – Journal Physics*, *95*, 1-8.

Asadpour, H., & Soleimani, H. R. (2014). Polarization dependence of optical bistability in the presence of external magnetic field. *Optics Communications*, *310*, 120-124.

Boller, K. -J., Imamoğlu, A., & Harris, S. E. (1991). Observation of electromagnetically induced transparency. *Physical Review Letters*, *66*(20), 2593-2596.

Brown, A., Joshi, A., & Xiao, M. (2003). Controlled steady-state switching in optical bistability. *Applied Physics Letters*, *83*(7), 1301-1303.

Cheng, D., Liu, C., & Gong, S. (2004). Optical bistability and multistability via the effect of spontaneously generated coherence in a three-level ladder-type atomic system. *Physics Letters A*, *332*(3-4), 244-249.

Gibbs, H. M., McCall, S. L., & Venkatesan, T. N. C. (1976). Differential gain and bistability using a sodium-filled Fabry-Perot interferometer. *Physics Review Letters*, *36*(19), 1135-1138.

Gong, S., Du, S., & Xu, Z. (1997). Optical bistability via atomic coherence. *Physics Letters A*, *226*, 293-297.

Gong, S., Du, S., Xu, Z., & Pan, S. (1996). Optical bistability via a phase fluctuation effect of the control field. *Physics Letters A*, *222*, 237-240.

Haifeng, X. (2019). Optical bistability and multistability via both coherent and incoherent fields in a three-level system. *Laser Physics*, *29*(1), 015205.

Harshawardhan, W., & Agarwal, G. S. (1996). Controlling optical bistability using electromagnetic-field-induced transparency and quantum interferences. *Physical Review A*, *53*, 1812-1817.

Hau, L. V., Harris, S. E., Dutton, Z., & Behroozi, C. H. (1999). Light speed reduction to 17 metres per second in an ultracold atomic gas. *Nature*, *397*, 594-598.

Hoang, M. D., & Nguyen, H. B. (2019). Controllable optical switching in a closed-loop three-level lambda system. *Physica Scripta, 94*(11), 115510.

Hoang, M. D., Luong, T. Y. N., & Nguyen, H. B. (2019). Optical switching and bistability in a degenerated two-level atomic medium under an external magnetic field. *Applied Optics, 58*(16), 4192-4199.

Hoang, M. D., Luong, T. Y. N., Dinh, X. K., & Nguyen, H. B. (2020). Controllable ultraslow optical solitons in a degenerated two-level atomic medium under EIT assisted by a magnetic field. *Scientific Reports, 10*(1), 15298.

Jafarzadeh, H., Sahrai, M., & Jamshidi-Ghaleh, K. (2014). Controlling the optical bistability in a Λ-type atomic system via incoherent pump field. *Applied Physics B, 117*, 927-933.

Joshi, A., Brown, A., Wang, H., & Xiao, M. (2003). Controlling optical bistability in a three-level atomic system. *Physical Review A, 67*, 041801.

Joshi, A., & Xiao, M. (2012). *Controlling steady-state and dynamical properties of atomic optical bistability*. World Scientific Publishing Co.

Joshi, A., Yang, W., & Xiao, M. (2003). Effect of quantum interference on optical bistability in the three-level V-type atomic system. *Physical Review A, 68*, 015806.

Ngo, Q. M., Le, K., & Lam, V. (2012). Optical bistability based on guided-mode resonances in photonic crystal slabs. *Journal of the Optical Society of America B, 29*(6), 1291-1295.

Ngo, Q. M., Kim, S., Lee, J., & Lim, H. (2012). All-optical switches based on multiple cascaded resonators with reduced switching intensity-response time products. *Journal of Lightwave Technology, 30*(22), 3525-3531.

Rosenberger, A. T., Orozco, L. A., & Kimble, H. J. (1983). Observation of absorptive bistability with two-level atoms in a ring cavity. *Physical Review A, 28*, 2569-2572.

Steck, D. A. (2019). *Rubidium 87 D line data* [White paper]. http://steck.us/alkalidata.

Yan, M., Rickey, E. G., & Zhu, Y. (2001). Observation of absorptive photon switching by quantum interference. *Physical Review A, 64*(4), 041801.

Zhang, D., Yu, R., Li, J., Ding, C., & Yang, X. (2013). Laser-polarization-dependent and magnetically controlled optical bistability in diamond nitrogen-vacancy centers. *Physics Letters A, 377*(38), 2621-2627.

Zibrov, A. S., Lukin, M. D., Nikonov, D. E., Hollberg, L., Scully, M. O., Velichansky, V. L., & Robinson, H. G. (1995). Experimental demonstration of laser oscillation without population inversion via quantum interference in Rb. *Physical Review Letters, 75*(8), 1499-1502.

APPENDIX

In this section, we derive the term ρ_{21} by solving the density matrix Equations (3) in the steady state. We set: $\tilde{\gamma}_{21} = -(i(\Delta_p + \Delta_B) + \gamma)$, $\tilde{\gamma}_{31} = -\left(\gamma_{31} + i\left(\Delta_p - \Delta_c + 2\Delta_B\right)\right)$, $\tilde{\gamma}_{23} = -\left(i\left(\Delta_c - \Delta_B\right) + \gamma\right)$.

From Equation (3e), we have:

$$\rho_{32} = \frac{\tilde{\gamma}_{31}\rho_{31} + i\Omega_c\rho_{21}}{i\Omega_p} \text{ and } \rho_{23} = \frac{-\tilde{\gamma}_{13}\rho_{13} + i\Omega_c\rho_{12}}{i\Omega_p}. \tag{A1}$$

Thus:

$$\rho_{32} - \rho_{23} = \frac{\tilde{\gamma}_{31}\rho_{31} + \tilde{\gamma}_{13}\rho_{13} + i\Omega_c\left(\rho_{21} - \rho_{12}\right)}{i\Omega_p}. \tag{A2}$$

From Equation (3b), we have:

$$\rho_{22} = \frac{i\Omega_p\left(\rho_{12} - \rho_{21}\right) + i\Omega_c\left(\rho_{32} - \rho_{23}\right)}{\gamma_{21} + \gamma_{23}} \tag{A3}$$

Substituting Equations (A2) and (A3) into Equation (3c), we obtain the population difference, $\rho_{33} - \rho_{22}$, as follows:

$$\rho_{33} - \rho_{22} = i\frac{\left(\gamma_{23} - \gamma_{31}\right)\Omega_p^2 + \left(\gamma_{21} + \gamma_{31}\right)\Omega_c^2}{\gamma_{31}\left(\gamma_{21} + \gamma_{31}\right)\Omega_p}\left(\rho_{12} - \rho_{21}\right) - \frac{\left(\gamma_{21} + \gamma_{31}\right)\left(\tilde{\gamma}_{13}\rho_{13} + \tilde{\gamma}_{31}\rho_{31}\right)\Omega_c}{\gamma_{31}\left(\gamma_{21} + \gamma_{31}\right)\Omega_p}, \tag{A4}$$

Substituting Equation (A4) into Equation (3f) and performing some transformations, we obtain:

$$\rho_{31} = \frac{i\left(MM_{123} + MM_{13} - M_{32}M_{123}\right)\rho_{21} + i\left(M_{13}M_{23} - MM_{123} - MM_{13}\right)\rho_{12}}{M_{123}M_{321} - M_{13}M_{31}}, \tag{A5}$$

where:

$$M_{123} = -\left(\gamma_{21} + \gamma_{31}\right)\tilde{\gamma}_{13}\Omega_c^2 + \left(\gamma_{21} + \gamma_{23}\right)\gamma_{31}\Omega_p^2 + \left(\gamma_{21} + \gamma_{23}\right)\gamma_{31}\tilde{\gamma}_{31}\tilde{\gamma}_{13} \tag{A6}$$

$$M_{23} = \gamma_{31}\left(\gamma_{21} + \gamma_{31}\right)\tilde{\gamma}_{23}\Omega_c \tag{A7}$$

$$M_{31} = \left(\gamma_{21} + \gamma_{31}\right)\tilde{\gamma}_{31}\Omega_c^2 \tag{A8}$$

$$M = \Omega_c\left[\left(\gamma_{23} - \gamma_{31}\right)\Omega_p^2 + \left(\gamma_{21} + \gamma_{31}\right)\Omega_c^2\right] \tag{A9}$$

Substituting Equation (A5) into Equation (3d) and using the initial conditions $\rho_{11}^{(0)} = \rho_{33}^{(0)} = 1/2; \rho_{22}^{(0)} = 0$, we obtain the density matrix element ρ_{21} as follows:

$$\rho_{21} = i\Omega_p \frac{\left\{ \begin{array}{l} \left(M_{123}M_{321} - M_{13}M_{31}\right) \\ -\left[\left(M_{123}M_{321} - M_{13}M_{31}\right) \times \dfrac{2\tilde{\gamma}_{12}\left(M_{123}M_{321} - M_{13}M_{31}\right) - 2\Omega_c\left(MM_{321} + MM_{31} - M_{23}M_{321}\right)}{2\Omega_c\left(M_{13}M_{23} + MM_{123} - MM_{13}\right)}\right] \end{array} \right\}}{\left\{ \begin{array}{l} \left[2\tilde{\gamma}_{12}\left(M_{123}M_{321} - M_{13}M_{31}\right) - 2\Omega_c\left(MM_{321} + MM_{31} - M_{23}M_{321}\right)\right] \\ \times\left[\dfrac{2\tilde{\gamma}_{21}\left(M_{123}M_{321} - M_{13}M_{31}\right) - 2\Omega_c\left(MM_{123} + MM_{13} - M_{32}M_{123}\right)}{2\Omega_c\left(M_{13}M_{23} + MM_{123} - MM_{13}\right)}\right] \\ -2\Omega_c\left(M_{31}M_{32} - MM_{321} - MM_{31}\right) \end{array} \right\}}, \quad \text{(A10)}$$

with the M_{kji} being complex conjugates of the M_{ijk}.

Putting the term ρ_{21} into Equation (8) and performing the investigation, we get the results shown in Section 3 of this paper.